Supplemental Information

Gibbs free-energy gradient along the path of glucose transport through human glucose transporter 3

Huiyun Liang, Allen K Bourdon, Liao Y Chen, Clyde F Phelix, George Perry

In this online-only supplemental information (SI), we include one movie (Movie S1) illustrating the process of hydrating a β-D-glucose (BGLC) and four movies (Movies S2 to S5) illustrating the facilitated diffusion of a BGLC through glucose transporter 3 (GLUT3).

We supplement the main study of β-D-glucose transport through GLUT3 with additional simulations that involve large conformational changes of GLUT3. In this part, we first implemented the large changes from the exofacial conformation to the endofacial conformation that GLUT3 has long been hypothesized to have (Fig. S1) when transporting a glucose from the extracellular fluid to the intracellular space. Using the endofacial conformation, we computed the free-energy profile from the binding site to the intracellular side (red curve in Fig. S2). This free-energy profile on the basis of the long-held hypothesis of large conformational changes also gives the Michaelis-Menten characteristics that are indistinguishable from what were obtained without forcing the large conformational changes (presented in the main text). Namely, there are no significant barriers in the free-energy profiles on either the extracellular or the intracellular side, leading to high Vmax and low Km. In this, our research does not validate/invalidate the long-held hypothesis for glucose transport through GLUT3 but elucidates the Michaelis-Menten characteristics in full agreement with experimental data.

We also include a study of α-D-glucose (AGLC) transport through GLUT3 in ways identical to the study of BGLC. The free-energy profile of AGLC is shown Fig.S3, which confirms that AGLC and BGLC have similar characteristics of transport through GLUT3. The AGLC-GLUT3 affinity is equal to the BGLC-GLUT3 affinity within the margin of error. Both glucose anomers have low Km and high Vmax in the Michaelis-Menten characteristics.

movieS1_hydrBGLC.avi

Movie S1. Hydration of BGLC. BGLC is pulled by its C1 and O5 atoms from vacuum into a body of water. BLGC is in large spheres colored by atom names (C, cyan; O, red; H, white). Waters are in ball-and-sticks colored by atom names.

movieS2_glut3extraview.avi

Movie S2. Facilitated diffusion of BGLC through GLUT3 viewed from the extracellular side. BGLC is in large spheres colored by atom names. GLUT3 is in cartoons colored by residue types (negatively charged, red; positively charged, blue; hydrophilic, green; hydrophobic, white). Lipids (not all shown) are in lines colored by atom names (in addition to the afore-listed: P, purple; N, blue).

movieS3_glut3intraview.avi

Movie S3. Facilitated diffusion of BGLC through GLUT3 viewed from the intracellular side. Representations identical to Movie S2.

movieS4_glut3sdvw.avi

Movie S4. Facilitated diffusion of BGLC through GLUT3 viewed from the membrane. Representations identical to Movie S2.

movieS5_waters-path.avi

Movie S5. Waters following BGLC along its transport path through GLUT3. BGLC is in large spheres colored by atom names. Waters are in licorices colored by atom names. GLUT3 is in ribbons colored by residue types.

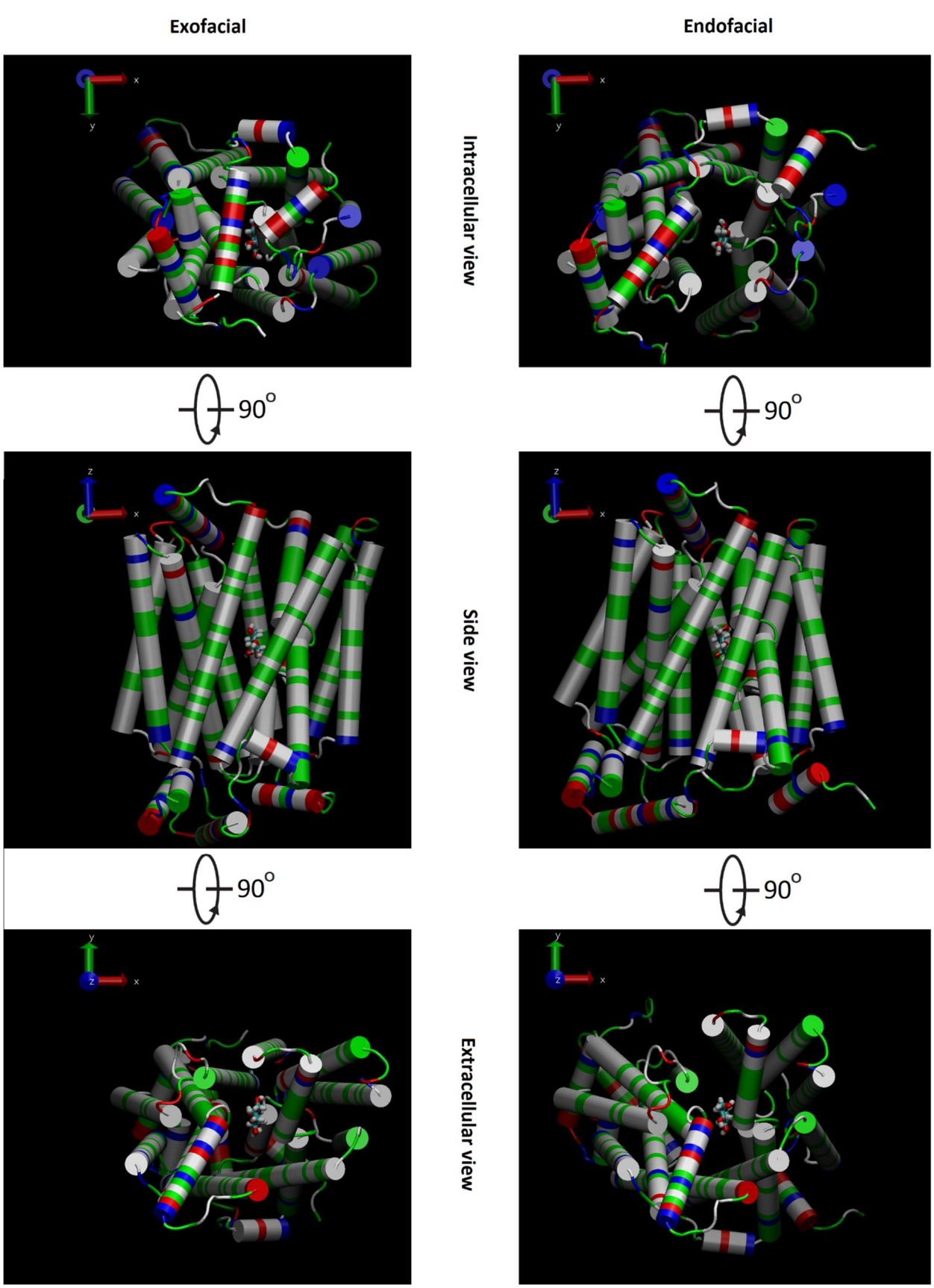
Exofacial
Endofacial
Intracellular view
90°
90°
Side view
90°
90°
Extracellular view

Fig. S1. GLUT3 in the exofacial (left column) and the endofacial (right column) conformations, viewed from the intracellular side (top row), the side (the plane of the membrane, middle row), and the extracellular side (bottom row). D-glucose is represented as licorices colored by atom names (O, red; N, blue; C, cyan; H, white). The protein is represented as cartoons colored by residue types (negatively charged, red; positively charged, blue; hydrophobic white; hydrophilic, green). The D-glucose was held in position at the binding site when GLUT3 was steered through the conformational changes. During the 50 ns steered MD run to pull GLUT3 from the exofacial conformation (three panels in the left column) to the endofacial conformation (three panels in the right column), two groups of alpha carbons on the intracellular end were steered away from each other: two alpha carbons (TRP386-αC and ALA390-αC) in the (1.0, -1.0, 0.0) direction and two alpha carbons (GLY143-αC and ARG151-αC) in the (-1.0, 1.0, 0.0) direction. Two groups on the extracellular end were pulled toward one another: two alpha carbons (Ala114-αC and GLU182-αC) in the (1.0, 0.0, 0.0) direction and two alpha carbons (LEU355-αC and ALA429-αC) in the (-1.0, 0.0, 0.0) direction. The pulling speeds were all at 0.1 Å/ns and the degrees of freedom perpendicular to the pulling directions were free (unconstrained).

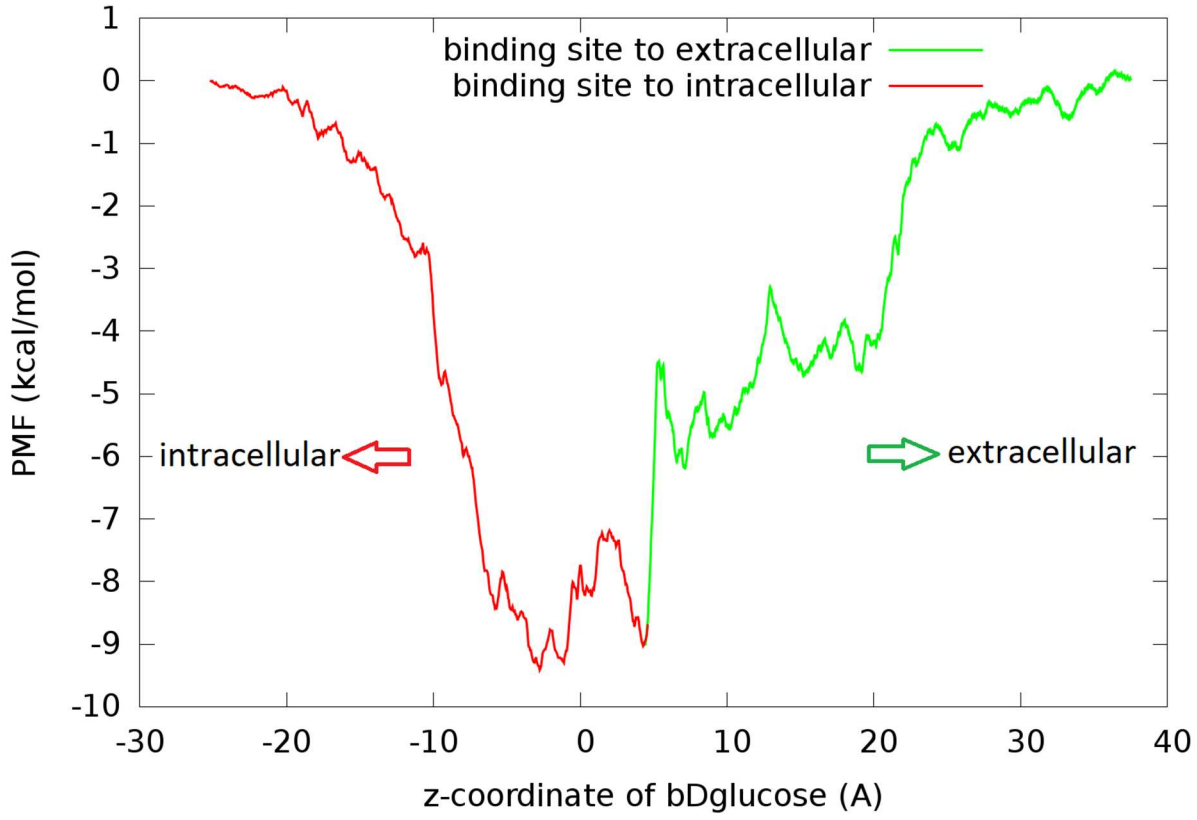

Fig. S2. Free-energy profile of β-D-glucose transport through GLUT3. The extracellular part of the transport path was computed using the exofacial conformation shown in Fig. S1, left panels. The intracellular part of the transport path was computed using the endofacial conformation shown in Fig. S1, right panels.

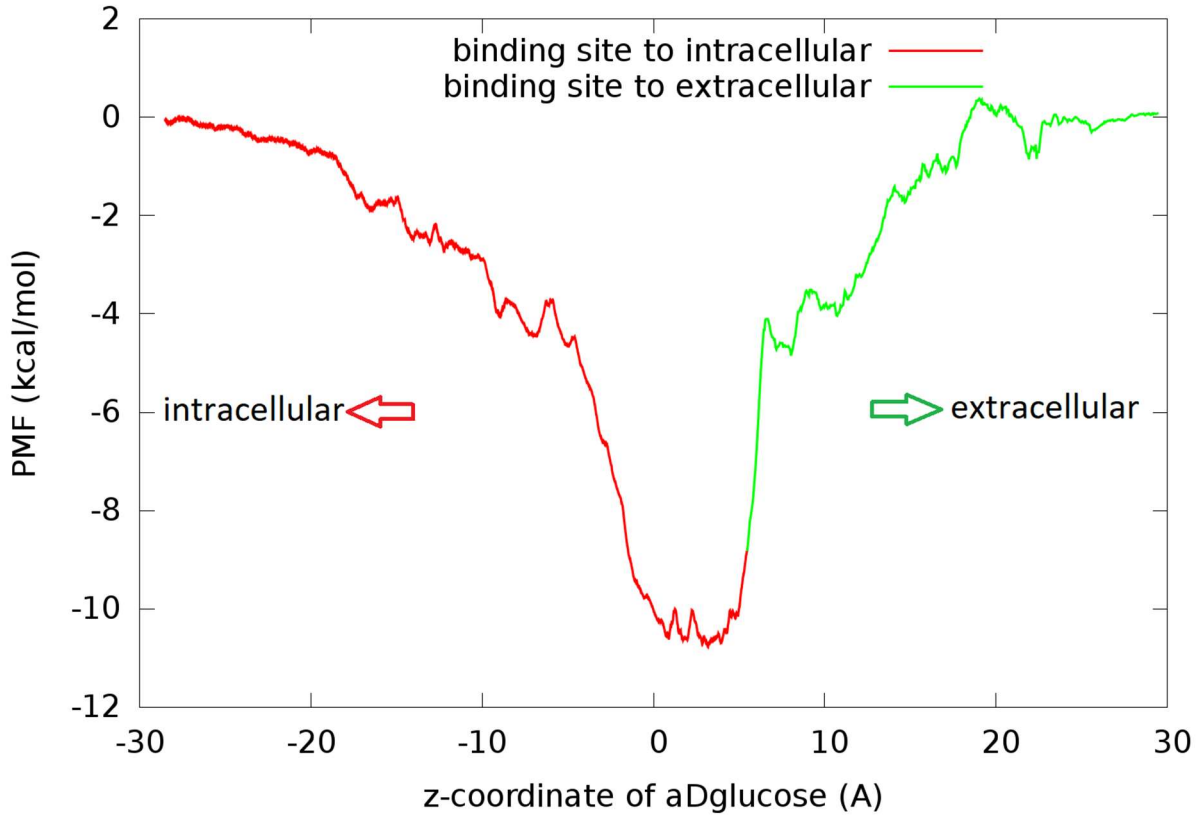

Fig. S3. Free-energy profile of α-D-glucose transport through GLUT3. The extracellular part of the transport path was computed using the exofacial conformation shown in Fig. S1, left panels. The intracellular part of the transport path was computed using the endofacial conformation shown in Fig. S1 right panels.